

*This copy is for your personal, non-commercial use only.*

If you wish to distribute this article to others, you can order high-quality copies for your colleagues, clients, or customers by [clicking here](#).

Permission to republish or repurpose articles or portions of articles can be obtained by following the guidelines [here](#).

**The following resources related to this article are available online at [www.sciencemag.org](http://www.sciencemag.org) (this information is current as of February 23, 2011):**

**Updated information and services**, including high-resolution figures, can be found in the online version of this article at:

<http://www.sciencemag.org/content/330/6012/1813.full.html>

**Supporting Online Material** can be found at:

<http://www.sciencemag.org/content/suppl/2010/11/22/science.1198366.DC1.html>

A list of selected additional articles on the Science Web sites **related to this article** can be found at:

<http://www.sciencemag.org/content/330/6012/1813.full.html#related>

This article **cites 22 articles**, 3 of which can be accessed free:

<http://www.sciencemag.org/content/330/6012/1813.full.html#ref-list-1>

This article has been **cited by** 1 articles hosted by HighWire Press; see:

<http://www.sciencemag.org/content/330/6012/1813.full.html#related-urls>

This article appears in the following **subject collections**:

Planetary Science

[http://www.sciencemag.org/cgi/collection/planet\\_sci](http://www.sciencemag.org/cgi/collection/planet_sci)

## References and Notes

1. L. Berger, *J. Appl. Phys.* **55**, 1954 (1984).
2. L. Berger, *Phys. Rev. B* **33**, 1572 (1986).
3. S. S. P. Parkin, M. Hayashi, L. Thomas, *Science* **320**, 190 (2008).
4. J. Grollier *et al.*, *Appl. Phys. Lett.* **83**, 509 (2003).
5. A. Yamaguchi *et al.*, *Phys. Rev. Lett.* **92**, 077205 (2004).
6. M. Yamanouchi, D. Chiba, F. Matsukura, H. Ohno, *Nature* **428**, 539 (2004).
7. N. Vernier, D. A. Allwood, D. Atkinson, M. D. Cooke, R. P. Cowburn, *Europhys. Lett.* **65**, 526 (2004).
8. M. Kläui *et al.*, *Phys. Rev. Lett.* **95**, 026601 (2005).
9. D. Ravelosona, D. Lacour, J. A. Katine, B. D. Terris, C. Chappert, *Phys. Rev. Lett.* **95**, 117203 (2005).
10. M. Hayashi *et al.*, *Phys. Rev. Lett.* **98**, 037204 (2007).
11. S. Yang, J. L. Erskine, *Phys. Rev. B* **75**, 220403 (2007).
12. G. Meier *et al.*, *Phys. Rev. Lett.* **98**, 187202 (2007).
13. M. Hayashi, L. Thomas, R. Moriya, C. Rettner, S. S. P. Parkin, *Science* **320**, 209 (2008).
14. G. Tataru, H. Kohno, *Phys. Rev. Lett.* **92**, 086601 (2004).
15. Z. Li, S. Zhang, *Phys. Rev. Lett.* **92**, 207203 (2004).
16. S. Zhang, Z. Li, *Phys. Rev. Lett.* **93**, 127204 (2004).
17. A. Thiaville, Y. Nakatani, J. Miltat, Y. Suzuki, *Europhys. Lett.* **69**, 990 (2005).
18. S. E. Barnes, S. Maekawa, *Phys. Rev. Lett.* **95**, 107204 (2005).
19. A. P. Malozemoff, J. C. Slonczewski, *Magnetic Domain Walls in Bubble Materials* (Academic Press, New York, 1979).
20. L. Thomas *et al.*, *Nature* **443**, 197 (2006).
21. R. Moriya *et al.*, *Nat. Phys.* **4**, 368 (2008).
22. I. M. Miron *et al.*, *Phys. Rev. Lett.* **102**, 137202 (2009).
23. T. A. Moore *et al.*, *Phys. Rev. B* **80**, 132403 (2009).
24. M. Eltschka *et al.*, *Phys. Rev. Lett.* **105**, 056601 (2010).
25. E. Saitoh, H. Miyajima, T. Yamaoka, G. Tataru, *Nature* **432**, 203 (2004).
26. D. Bedau *et al.*, *Phys. Rev. Lett.* **99**, 146601 (2007).
27. L. Thomas *et al.*, *Science* **315**, 1553 (2007).
28. L. Bocklage *et al.*, *Phys. Rev. B* **78**, 180405 (2008).
29. Materials and methods can found as supporting material on Science Online.
30. The rise and fall times of the shift current pulses, measured in a transmission geometry through the devices using a real-time oscilloscope and corresponding to a variation of 20/80% of the pulse amplitude, were ~0.5 ns.
31. M. Hayashi *et al.*, *Phys. Rev. Lett.* **97**, 207205 (2006).
32. V. Vlaminck, M. Bailleul, *Science* **322**, 410 (2008).
33. We thank S.-H. Yang, X. Jiang, and B. Hughes for useful discussions and help with sample fabrication.

## Supporting Online Material

www.sciencemag.org/cgi/content/full/330/6012/1810/DC1  
Materials and Methods  
Figs. S1 to S3  
References

7 September 2010; accepted 16 November 2010  
10.1126/science.1197468

# Cassini Finds an Oxygen–Carbon Dioxide Atmosphere at Saturn’s Icy Moon Rhea

B. D. Teolis,<sup>1\*</sup> G. H. Jones,<sup>2,3</sup> P. F. Miles,<sup>1</sup> R. L. Tokar,<sup>4</sup> B. A. Magee,<sup>1</sup> J. H. Waite,<sup>1</sup> E. Roussos,<sup>5</sup> D. T. Young,<sup>1</sup> F. J. Crary,<sup>1</sup> A. J. Coates,<sup>2,3</sup> R. E. Johnson,<sup>6</sup> W.-L. Tseng,<sup>6</sup> R. A. Baragiola<sup>6</sup>

The flyby measurements of the Cassini spacecraft at Saturn’s moon Rhea reveal a tenuous oxygen (O<sub>2</sub>)–carbon dioxide (CO<sub>2</sub>) atmosphere. The atmosphere appears to be sustained by chemical decomposition of the surface water ice under irradiation from Saturn’s magnetospheric plasma. This in situ detection of an oxidizing atmosphere is consistent with remote observations of other icy bodies, such as Jupiter’s moons Europa and Ganymede, and suggestive of a reservoir of radiolytic O<sub>2</sub> locked within Rhea’s ice. The presence of CO<sub>2</sub> suggests radiolysis reactions between surface oxidants and organics or sputtering and/or outgassing of CO<sub>2</sub> endogenic to Rhea’s ice. Observations of outflowing positive and negative ions give evidence for pickup ionization as a major atmospheric loss mechanism.

On 2 March 2010, the Cassini spacecraft executed a flyby of Saturn’s icy moon Rhea, with a trajectory inbound toward Saturn passing 97 km over the surface at 81° north latitude. The Ion Neutral Mass Spectrometer (INMS)—a quadrupole mass analyzer equipped with an antechamber and electron-impact ionizer for in situ collection and detection of neutral gas (1)—was operated during the flyby with the antechamber inlet pointed favorably at an angle of 44° to Cassini’s trajectory, enabling the measurement of neutral species. INMS detected a tenuous atmosphere of oxygen and carbon dioxide in mass channels 32 and 44 daltons, reaching peak densities along the trajectory of 5 and 2 ± 1 × 10<sup>10</sup> molecules per m<sup>3</sup>, respectively. A highly non-uniform

atmosphere was observed, with the CO<sub>2</sub> seen almost exclusively on the outbound portion of the trajectory over the day-lit hemisphere (Fig. 1). In contrast, the O<sub>2</sub> profile is more symmetrical about the point of closest approach, but it is nevertheless shifted slightly outbound to the day side (Fig. 1).

Spectra from the Cassini Plasma Spectrometer (CAPS) (2), acquired during the more distant 502- and 5736-km flybys on 26 November 2005 and 30 August 2007, also show clear signatures (Fig. 2) symptomatic (3) of outflowing streams of positive and negative ions, which are produced by ionization of the atmosphere and electron capture, respectively. These ions are subsequently swept up into Saturn’s rotating magnetosphere (4). The timing of the positive and negative ion signatures inbound and outbound from Rhea (Fig. 2) is consistent with the expected  $\vec{E} \times \vec{B}$  cycloidal trajectories (where  $\vec{E}$  and  $\vec{B}$  are the electric and magnetic fields, respectively) of pickup ions in the mass ranges of 26 to 56 daltons (possibly O<sub>2</sub><sup>+</sup> or CO<sub>2</sub><sup>+</sup>) and 13 to 26 daltons, respectively; thus, we tentatively identify the negative species as O<sup>-</sup>. The mass uncertainty results from the CAPS energy and angular resolution (2), as well as the still-uncertain corotation electric field and corotation speed in Rhea’s plasma wake (5). Unlike the 2005 encounter, only positive ions were detected during the 11 times more distant 2007 flyby, suggesting rapid (6) removal of

loosely bound electrons from the negative ions by photo or electron impact ionization as the ions move away from Rhea.

The in situ detection of O<sub>2</sub> and CO<sub>2</sub> at Rhea is consistent with remote observations of Jupiter’s icy moons, where the Galileo spacecraft’s Near-Infrared Mapping Spectrometer observed resonantly scattered 4.26-μm infrared emission from atmospheric CO<sub>2</sub> at Callisto (7), and the Hubble Space Telescope measured 1304 and 1356 Å ultraviolet fluorescence from electron-impact dissociatively excited atmospheric O<sub>2</sub> at Europa and Ganymede (8). Oxygen at Europa and Ganymede is generated by radiation chemistry and sputtered from the surface ice into the atmosphere by bombarding ions and electrons from Jupiter’s magnetosphere (8). The Jupiter findings, and the detection by Cassini of O<sub>2</sub> from ultraviolet (UV) photodecomposition of ice in Saturn’s rings (9), have long suggested the possibility of oxygen atmospheres around the saturnian icy satellites (10), which orbit inside Saturn’s magnetosphere. Ganymede’s ice (11) and that of Europa and Callisto (12) also exhibit the weak 5770 and 6275 Å optical absorption signatures of trapped radiolytic O<sub>2</sub> (13), which has been shown in laboratory experiments to lead to ozone as a by-product (14), along with eventual O<sub>2</sub> ejection from the surface through sputtering (15). Rhea and Saturn’s icy moon Dione are especially interesting because O<sub>3</sub> is present in their surface ices (16), a trait that they share with Ganymede (17). Together with the existence of ozone in Rhea’s ice, the detection of an O<sub>2</sub> atmosphere is consistent with surface radiolysis, as seen at other icy satellites, and indicative of O<sub>2</sub> trapped in the surface ice.

On the basis of CAPS and Magnetospheric Imaging Instrument (MIMI) measurements of the saturnian ion and electron plasma, as well as updated laboratory estimates of O<sub>2</sub> production and desorption from ice irradiated with different projectiles and energies, we have modeled the expected production of O<sub>2</sub> from different radiation sources (18). The principal oxygen source in the model is bombardment by water group ions (W<sup>+</sup>) from Saturn’s corotating plasma (Table 1), which sweep past Rhea along its orbit while preferentially bombarding its trailing hemisphere. The oxygen is, therefore, produced preferentially on the

<sup>1</sup>Southwest Research Institute, Space Science and Engineering Division, 6220 Culebra Road, San Antonio, TX 78238, USA.

<sup>2</sup>Mullard Space Science Laboratory, Department of Space and Climate Physics, University College London (UCL), Holmbury St. Mary, Dorking, Surrey RH5 6NT, UK. <sup>3</sup>The Centre for Planetary Sciences at UCL/Birkbeck, Gower Street, London WC1E 6BT, UK.

<sup>4</sup>Los Alamos National Laboratory, Space Science and Applications, Los Alamos, NM 87545, USA. <sup>5</sup>Max-Planck-Institut für Sonnensystemforschung, Max-Planck-Strasse 2, 37191 Katlenburg-Lindau, Germany. <sup>6</sup>University of Virginia, Department of Materials Science and Engineering, 116 Engineer’s Way, Charlottesville, VA 22903, USA.

\*To whom correspondence should be addressed. E-mail: ben.teolis@swri.org

**Fig. 1.** (A) INMS 32-dalton measurement (32) of the O<sub>2</sub> density along Cassini's trajectory versus time during the 2 March 2010 Rhea encounter. The black vertical dotted line indicates that the closest approach (CA) was 17:40:39 UT at 96.8-km altitude and nearly simultaneous (later by ~0.05 s) with solar terminator traversal to Rhea's day side. The blue dashed curve denotes along-track density predicted by a Monte Carlo simulation of the O<sub>2</sub> atmosphere that assumes 100/40 K day/night surface temperatures, respectively (25). (B) Same as (A) for CO<sub>2</sub> in the 44-dalton mass channel. (C) Diagrammatic equatorial view of Rhea looking perpendicular to the Cassini 2010 trajectory (red line in Rhea's reference frame) on the same time scale as in (A) and (B). The vantage point at 81.8° longitude and 8.9° north latitude is near the apex (90° longitude) of Rhea's leading hemisphere. Cassini's motion toward Saturn at 8.6 km/s was nearly perpendicular (at 88.8°) to the day-night terminator (shown at the time of CA), with CA at 81.1° north latitude, 263.4° longitude. Rhea's orbit and Saturn's corotation direction point out of the page and perpendicular to the magnetic and corotation electric fields  $\vec{B}$  and  $\vec{E}$ . Also shown is the O<sub>2</sub> density cross section predicted by the Monte Carlo model.

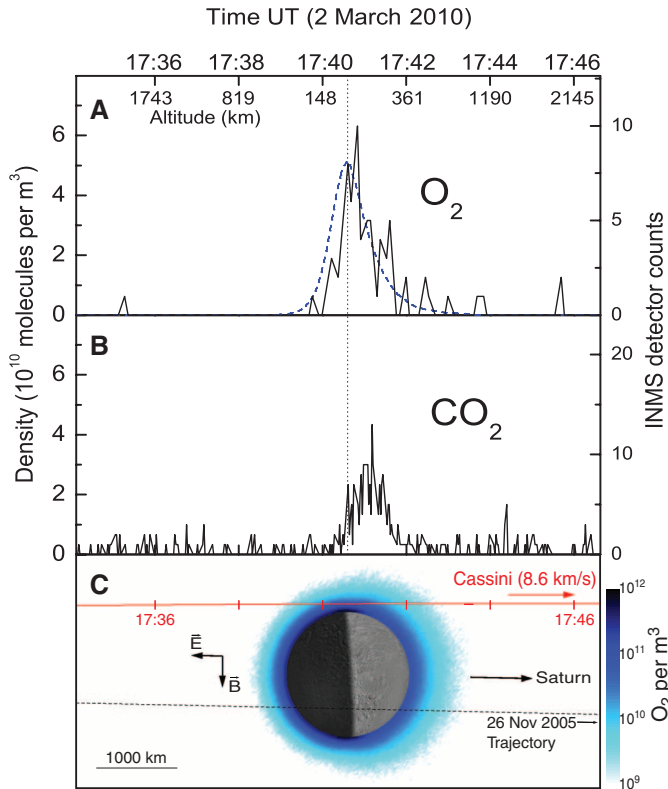
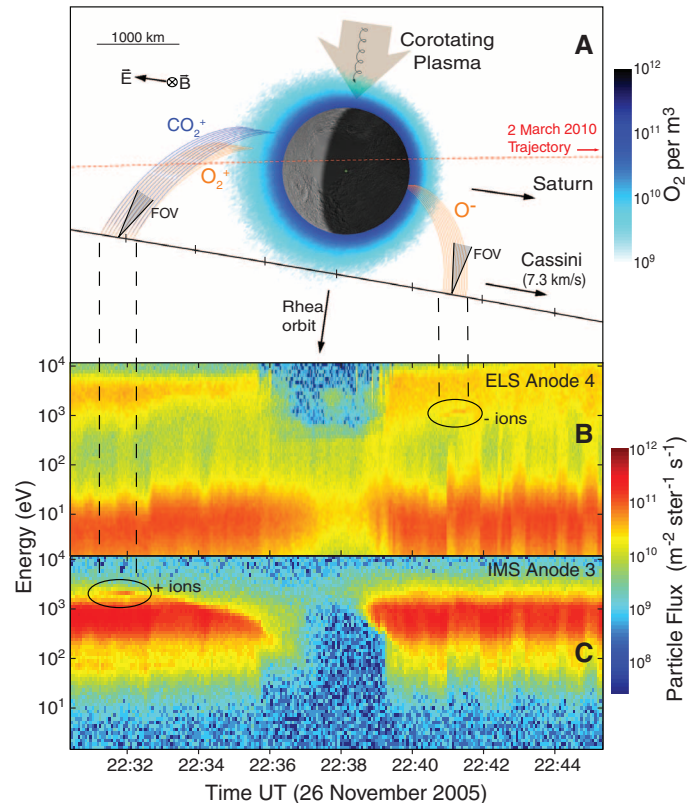


**Fig. 2.** (A) Diagrammatic Rhea north polar view with the 26 November 2005 Cassini flyby trajectory (black line in Rhea's reference frame) during which CAPS detected pickup ions. The time scale is matched to that of (B) and (C). The day and night hemispheres are shown during CA at 22:37:39 UT. The trajectory traversed Rhea's plasma wake, with CA at 502-km altitude, 226 km south (Fig. 1) of the equator. Our model prediction of the O<sub>2</sub> density (226-km south cross section) is also shown. The O<sub>2</sub><sup>+</sup> and O<sup>-</sup> (orange) and CO<sub>2</sub><sup>+</sup> trajectories (blue) are those required to enter anodes 4 and 3 (33) of the CAPS Electron Spectrometer (ELS) and Ion Mass Spectrometer (IMS) at the time and energy of the ion signatures. The trajectories assume (in Saturn's reference frame) a  $\vec{B}$  of 26 nT (34) and a corotation electric field  $\vec{E}$  [within uncertainty (5)] of 1.77 (O<sub>2</sub><sup>+</sup>, O<sup>-</sup>) or 1.51 (CO<sub>2</sub><sup>+</sup>) V/km. Before ionization, most atmospheric neutrals have thermal speeds less than 1 km/s, so  $|\vec{E}|$  is optimized such that ions backtracked from Cassini come nearly to rest (the trajectory starting point). FOV, field of view. (B) ELS negative particle flux spectrogram from anode 4 (20° FOV), which had optimal pointing. Negative pickup ions are indicated by the sharp feature near 22:41 UT ( $\pm 0.35$  min) and 1.14 ( $\pm 0.15$ ) keV over the electron background. (C) Positive ions from IMS anode 3: Pickup ions produce the sharp 22:32 UT ( $\pm 0.5$  min), 2.06 ( $\pm 0.2$ )-keV signature over the background of (mostly) corotating H<sup>+</sup>/W<sup>+</sup> (31).



trailing hemisphere. Relative to the amount of energy deposited by the different radiation sources, the W<sup>+</sup> ions are also the most efficient O<sub>2</sub> producers (Table 1). Because of their mass, these ions are the most effectively stopped on impact within the ice; that is, they deposit the most energy close to the material surface where, according to experiments, O<sub>2</sub> synthesis is favored most (18). The predicted total global production rate of  $\sim 2.2 \times 10^{24}$  O<sub>2</sub> molecules per second is within the  $\sim 0.4$  to  $4 \times 10^{24} \text{ s}^{-1}$  range implied by the elevated O<sub>2</sub><sup>+</sup> densities seen by CAPS near Rhea's orbit (19).

In contrast to O<sub>2</sub>, knowledge of Rhea's CO<sub>2</sub> source is much less well constrained. Atmospheric CO<sub>2</sub> might result from sputtering of primordial CO<sub>2</sub> in Rhea's ice or from radiolysis reactions between surface water molecules, radiolytic oxygen, and carbonaceous minerals or organics possibly present in the surface ice (13, 20, 21) and/or deposited by micrometeorite bombardment (22). The trailing hemispheres of Rhea and Dione both show a darkening in their visible-infrared reflectance spectrum, which is indicative of such non-ice material. At Dione, the Cassini Visible and Infrared Mapping Spectrometer (VIMS) detected the 4.26- $\mu\text{m}$  absorption of CO<sub>2</sub> in the dark regions (22). However, the Rhea measurements are inconclusive: A possible detection of the CO<sub>2</sub> absorption in Rhea's global spectrum (22) was not confirmed in subsequent VIMS mapping measurements (23) of the surface. A completely endogenic CO<sub>2</sub> source is also possible: for instance, outgassing of primordial CO<sub>2</sub> or of CO<sub>2</sub> produced by aqueous chemistry from Rhea's interior, similar to scenarios suggested at Enceladus (24) and Callisto (7).

**Table 1.** Estimated O<sub>2</sub> production from different radiation sources.

Radiation source	Energy deposition (× 10 <sup>26</sup> eV/s)	Estimated O <sub>2</sub> production (× 10 <sup>22</sup> O <sub>2</sub> /s)
W <sup>+</sup>	14.8	170
H <sup>+</sup>	9.5	7.4
Electrons	73	38
Solar UV	8.1	4.2
Total	105	220

The surface source processes compete with atmospheric loss mechanisms to determine the atmospheric O<sub>2</sub> and CO<sub>2</sub> abundances. The loss mechanisms are Jeans escape and atmosphere-plasma interactions—that is, ionization, dissociation, charge exchange, and electron capture. The plasma-interaction channels result in fast neutral and ionized species that, depending on their point of origin (Fig. 2), either (i) collide with Rhea's surface (and implant into the ice or adsorb or react on the surface) or (ii) escape into space directly or (for ions) by  $\vec{E} \times \vec{B}$  pickup, as seen by CAPS.

We used a Monte Carlo approach to model the atmosphere by initializing O<sub>2</sub> molecules according to the expected surface position-dependent production (18) while allowing the molecules to execute random ballistic trajectories between surface impacts. The simulation assumed no surface adsorption, thermally equilibrated molecules with the surface on impact by reinitializing the speed with a Maxwell-Boltzmann distribution at the local surface temperature (25), and destroyed the molecules in mid-flight, according to the loss rate from plasma interactions or on leaving the Hill sphere (Jeans escape).

Our model predicts a day-side bulge due to the higher (25) temperatures (and, therefore, increased scale height) that is well matched by the outbound O<sub>2</sub> tail seen by INMS (Fig. 1); i.e., the warmer day-side temperatures expand the atmospheric gas to the altitude of Cassini's trajectory in this hemisphere. The bulge is also consistent with the predicted origin of the positive pickup ions at high altitudes during the 2005 flyby (Fig. 2). Non-negligible night-side O<sub>2</sub> adsorption could account (26) for the model's slight overestimate of the INMS inbound measurements (Fig. 1). The mean free path is ~6 to 30 × 10<sup>3</sup> km at the predicted day-night surface densities of ~9 to 40 × 10<sup>10</sup> O<sub>2</sub> m<sup>-3</sup> (26); therefore, the atmosphere can be considered as collisionless. The estimated Jeans escape of 6(±1) × 10<sup>22</sup> O<sub>2</sub> s<sup>-1</sup> is ~2.7% of the estimated total O<sub>2</sub> produced (~2.2 × 10<sup>24</sup> O<sub>2</sub> s<sup>-1</sup>), with the remainder lost because of plasma interactions and pickup. The total atmospheric O<sub>2</sub> abundance is estimated to be 2.5(±0.5) × 10<sup>29</sup> molecules, corresponding to an average atmospheric molecule lifetime of ~10<sup>5</sup> seconds, or ~1 day.

Whereas for O<sub>2</sub> the sticking times are short, CO<sub>2</sub> is much less volatile (27); thus, the night side could act as a much more effective cold trap for CO<sub>2</sub> condensation, possibly explaining the almost nonexistent CO<sub>2</sub> signal inbound on the night side

(Fig. 1). Locally condensed CO<sub>2</sub> would be re-released by solar heating as the dawn terminator advances across the surface, although some CO<sub>2</sub> might be trapped for longer periods in shadowed polar regions [analogous to lunar (28) volatiles]. Although surface CO<sub>2</sub> on the night side would be undetectable by Cassini VIMS (which measures reflected sunlight), CO<sub>2</sub> near the faintly illuminated poles or dawn terminator might be observable.

The estimated mean atmospheric O<sub>2</sub> column density of 3.4(±0.7) × 10<sup>16</sup> m<sup>-2</sup> over Rhea's surface is two orders of magnitude below the 2.4 to 14 and 1 to 10 × 10<sup>18</sup> m<sup>-2</sup> abundances at Europa and Ganymede (8), respectively, a difference likely attributable to the greater O<sub>2</sub> desorption flux from the warmer and more intensely irradiated Galilean satellites (29). Rhea's atmospheric abundance is also well below the 10<sup>18</sup> m<sup>-2</sup> detection limit of MIMI and the Cassini Ultraviolet Imaging Spectrograph, explaining why earlier attempts by these instruments to detect an atmosphere remotely were unsuccessful (30). In comparison, laboratory measurements on irradiated ice imply that 10<sup>19</sup> to 10<sup>20</sup> O<sub>2</sub> m<sup>-2</sup> (14, 15) are synthesized by penetrating ions as trapped molecules inside the bulk H<sub>2</sub>O solid, from which diffusive loss is expected to be slow; thus, it is likely that a large fraction of Rhea's oxygen is actually locked inside the moon's ice. The laboratory column densities correspond to ~0.4 to 4 × 10<sup>4</sup> metric tons of trapped O<sub>2</sub> globally on Rhea, but these are a lower limit because diffusion and micrometeorite gardening can disperse O<sub>2</sub> into the subsurface ice.

#### References and Notes

- J. H. Waite Jr. et al., *Space Sci. Rev.* **114**, 113 (2004).
- D. T. Young et al., *Space Sci. Rev.* **114**, 1 (2004).
- A. J. Coates et al., *Icarus* **206**, 618 (2010).
- CAPS did not detect pickup ions during the 2010 flyby because Cassini's path north of Rhea did not intersect the allowable ion trajectories (Figs. 1 and 2).
- Field strengths of 1.77 and 1.51 V/km, consistent with O<sub>2</sub><sup>+</sup> and CO<sub>2</sub><sup>+</sup> (Fig. 2), yield bulk plasma speeds |E|/|B| = 68 and 58 km/s, respectively, both of which are compatible with published estimates (31) and supplemental reference 44 (S44).
- Assuming a 49-km/s bulk plasma speed with respect to Rhea (18, 31), pickup ions reaching Cassini's 2007 position are approximately 2 min old, compared with ages of 10 (±5) s in 2005.
- R. W. Carlson, *Science* **283**, 820 (1999).
- D. T. Hall, P. D. Feldman, M. A. McGrath, D. F. Strobel, *Astrophys. J.* **499**, 475 (1998).
- W.-L. Tseng, W.-H. Ip, R. E. Johnson, T. A. Cassidy, M. K. Elrod, *Icarus* **206**, 382 (2010).
- J. Saur, D. F. Strobel, *Astrophys. J.* **620**, L115 (2005).
- J. R. Spencer, W. M. Calvin, M. J. Person, *J. Geophys. Res.* **100**, 19049 (1995).
- J. R. Spencer, W. M. Calvin, *Astron. J.* **124**, 3400 (2002).
- J. Spencer, *Icarus* **136**, 349 (1998).
- B. D. Teolis, M. J. Loeffler, U. Raut, M. Fama, R. A. Baragiola, *Astrophys. J.* **644**, L141 (2006).
- B. D. Teolis, J. Shi, R. A. Baragiola, *J. Chem. Phys.* **130**, 134704 (2009).
- K. S. Noll, T. L. Roush, D. P. Cruikshank, R. E. Johnson, Y. J. Pendleton, *Nature* **388**, 45 (1997).
- K. S. Noll, R. E. Johnson, A. L. Lane, D. L. Domingue, H. A. Weaver, *Science* **273**, 341 (1996).
- Materials, methods, and further discussion are available as supporting material on Science Online.
- CAPS measurements throughout the Saturn system imply an average relative O<sub>2</sub><sup>+</sup>/W<sup>+</sup> density of 0.31 ± 0.01% at 4.5 to

- 7.5R<sub>S</sub> (where R<sub>S</sub> is the radius of Saturn) from photo-ionization of ring-atmosphere O<sub>2</sub> and a statistically greater 0.41 ± 0.02% at 7.5 to 10.5R<sub>S</sub> (S45). Rhea orbits at 8.75R<sub>S</sub>.
- D. P. Cruikshank et al., *Icarus* **206**, 561 (2010).
- D. P. Cruikshank et al., *Icarus* **175**, 268 (2005).
- R. N. Clark et al., *Icarus* **193**, 372 (2008).
- K. Stephan et al., in *40th Lunar and Planetary Science Conference*, Abstract 1377 (Lunar and Planetary Institute, The Woodlands, TX, 23 to 27 March 2009).
- C. R. Glein, M. Y. Zolotov, E. L. Shock, *Icarus* **197**, 157 (2008).
- Considering the day/night hemisphere orientation at the times of the 2 March 2010 and 26 November 2005 flybys, we reconstructed a temperature map based on Cassini Composite Infrared Spectrometer (CIRS) measurements (S16) showing 100/40 K max/min day/night temperatures, respectively. Because the CIRS coverage did not include the poles, we assume a constant 35/75 K (26 Nov 2005, Saturn winter) and 35/35 K (2 March 2010, near Saturn equinox) beyond 75° north/south latitude.
- The predicted day-night surface densities correspond to surface pressures of 1.2 and 2.2 × 10<sup>-12</sup> mbar at 100 and 40 K, respectively. The values are 100 × 10<sup>10</sup> O<sub>2</sub>/m<sup>3</sup>, 4.8 × 10<sup>-12</sup> mbar, and 3 × 10<sup>3</sup> km mean free path for 35 K minimum at the poles. Any night-side or polar O<sub>2</sub> adsorption [e.g., into the porous surface regolith (S46)] would lower the overlying atmospheric density (Fig. 1); hence, the night-side and polar values are upper limits.
- The O<sub>2</sub> and CO<sub>2</sub> sublimation energies are 0.095 eV (S47) and 0.271 eV (S48) from the pure solid. Extrapolation from available equilibrium vapor pressure data (S49, S50) yields O<sub>2</sub> and CO<sub>2</sub> values of 5.69 × 10<sup>-5</sup> and 3.15 × 10<sup>-32</sup> mbar at 35 K, as well as 2547 and 2.11 × 10<sup>-4</sup> mbar at 100 K.
- J. M. Sunshine et al., *Science* **326**, 565 (2009); 10.1126/science.1179788.
- Compared with Rhea [40 to 100 K (S16)], the warmer Europa/Ganymede ice [80 to 132 K/90 to 152 K (S51, S52)] is expected to exhibit O<sub>2</sub> yields roughly one order of magnitude greater (15). For instance, Europa receives a mean of ~1.2 and 3.6 × 10<sup>17</sup> eV/m<sup>2</sup>/s (S53) from ions (H<sup>+</sup>, W<sup>+</sup>, S<sup>+</sup>) and electrons, respectively, and mean O<sub>2</sub> sources are ~10<sup>13</sup> to 10<sup>15</sup> O<sub>2</sub>/m<sup>2</sup>/s for both moons (S24–S28), which exceed the Rhea values: ~3.3 (ions) and 9.9 (electrons) × 10<sup>14</sup> eV/m<sup>2</sup>/s and 3.0 × 10<sup>11</sup> O<sub>2</sub>/m<sup>2</sup>/s.
- G. H. Jones et al., *Science* **319**, 1380 (2008).
- R. J. Wilson, R. L. Tokar, W. S. Kurth, A. M. Persoon, *J. Geophys. Res.* **115**, A05201 (2010).
- Mass channels are sampled one at a time by integrating detector counts during 0.031-s intervals. During the 2010 flyby, CO<sub>2</sub> and O<sub>2</sub> were sampled every 2.3 and 6.9 s, respectively.
- We assumed ions entering the center of the field of view, which is 20°.
- K. K. Khurana, C. T. Russell, M. K. Dougherty, *Icarus* **193**, 465 (2008).
- We thank E. Roussos, D. Mitchell, and the Cassini MIMI team for providing the MIMI data used in Figs. S1 and S4 and N. G. Petrik, A. G. Kavetsky, and G. A. Kimmel at Pacific Northwest National Laboratory, Richland, Washington, USA, for contributing the O<sub>2</sub> electron-stimulated desorption measurements in Fig. S9. The INMS and CAPS teams acknowledge support from NASA and the Jet Propulsion Laboratory under SwRI subcontracts 1283095 and 1356497, respectively. G.H.J. and A.J.C. acknowledge support for CAPS-ELS operations and analysis by the United Kingdom Space Agency, and G.H.J. was supported by a UK Science and Technology Facilities Council Advanced Fellowship. B.D.T. and R.A.B. acknowledge support by the NSF Astronomy and Astrophysics Program through grant AST0807830.

#### Supporting Online Material

www.sciencemag.org/cgi/content/full/science.1198366/DC1  
Materials and Methods  
SOM Text  
Figs. S1 to S10  
References and Notes

28 September 2010; accepted 12 November 2010  
Published online 25 November 2010;  
10.1126/science.1198366